frontiers in Soil Science

TYPE Original Research
PUBLISHED 02 October 2026
DOI 10.3389/fsoil.2026.1950823

Check for updates

OPEN ACCESS

EDITED BY
Federica Tamburini,
ETH Zürich, Switzerland

REVIEWED BY
Juan Ignacio Vilchez Morillas,
Universidade Nova de Lisboa, Portugal
Chengming Zhang,
Hokkaido University, Japan

*CORRESPONDENCE
Martina Mazzon
martina.mazzon2@unibo.it

RECEIVED 28 July 2026
REVISED 02 September 2026
ACCEPTED 03 September 2026
PUBLISHED 02 October 2026

CITATION
Gioacchini P, Mazzon M, Guerrini S, Alberoni D, Cupi J, Di Gioia D and Marzadori C (2026) Contrasting responses of loamy and sandy soils to biodegradable plastic residues: microbial biomass, aggregation, and aggregate-associated carbon and nitrogen. *Front. Soil Sci.* 6:1950823. doi: 10.3389/fsoil.2026.1950823

COPYRIGHT
© 2026 Gioacchini, Mazzon, Guerrini, Alberoni, Cupi, Di Gioia and Marzadori. This is an open-access article distributed under the terms of the Creative Commons Attribution License (CC BY). The use, distribution or reproduction in other forums is permitted, provided the original author(s) and the copyright owner(s) are credited and that the original publication in this journal is cited, in accordance with accepted academic practice. No use, distribution or reproduction is permitted which does not comply with these terms.

Contrasting responses of loamy and sandy soils to biodegradable plastic residues: microbial biomass, aggregation, and aggregate-associated carbon and nitrogen

Paola Gioacchini, Martina Mazzon*, Sara Guerrini, Daniele Alberoni, Joana Cupi, Diana Di Gioia and Claudio Marzadori

Department of Agricultural and Food Sciences, Alma Mater Studiorum – University of Bologna, Bologna, Italy

Soil-biodegradable plastic (BDP) mulches are increasingly used as alternatives to conventional plastic films because they can be incorporated into soil after use. However, their degradation introduces an exogenous carbon source that may affect microbial activity, soil aggregation, and carbon (C) and nitrogen (N) stabilization. This study investigated the effects of increasing BDP doses on microbial biomass carbon (MBC), bacterial 16S rRNA gene-copy abundance, and fungal target-gene abundance, aggregate-size distribution, and aggregate-associated C, N, $\delta^{13}C$, and $\delta^{15}N$ in a loamy and a sandy soil. The soils were incubated for one year with BDP fragments at 100, 1, 000, and 10, 000 mg kg^{-1} soil, corresponding to 0.01, 0.1, and 1% w/w, respectively. Microbial biomass C and bacterial and fungal target-gene abundance were assessed during incubation, while macroaggregates, microaggregates, and the silt–clay fraction were separated at the end of the experiment. The highest BDP dose induced responses in both soils, increasing microbial biomass C by 69% in the loamy soil and 25% in the sandy soil relative to their respective controls after one year. This treatment also increased macroaggregate abundance by 32% and 11% in the loamy and sandy soils, respectively, while decreasing the free silt–clay fraction. These changes were accompanied by higher C and N contents in macroaggregates, and also in sandy-soil microaggregates. Lower BDP doses produced weaker and more soil-specific effects, including increased microaggregate recovery in the loamy soil. $\delta^{15}N$ progressively increased from macroaggregates to finer fractions in both soils, but was not affected by the presence of BDP. In contrast, $\delta^{13}C$ enrichment toward finer fractions occurred only in the loamy soil, demonstrating that soil characteristics, such as texture, may regulate C transformation and potential stabilization. Overall, BDP effects were dose-dependent and potentially modulated by soil properties. Although the strongest responses occurred at a concentration exceeding realistic annual inputs, detectable effects at lower doses highlight the need for long-term field studies evaluating repeated BDP incorporation.

KEYWORDS
carbon and nitrogen stabilization, microbial biomass, soil aggregates, soil-biodegradable mulch, stable isotopes

1 Introduction

Plastic mulches are widely used in agriculture because they can enhance crop productivity by suppressing weeds, increasing soil temperature, conserving soil moisture and nutrients, and extending the growing season (1–5). However, conventional plastic mulches must be removed and properly disposed of at the end of their functional lifespan. Incomplete recovery and improper disposal may result in their persistence and progressive fragmentation into microplastics, which can disperse throughout terrestrial and aquatic environment (6, 7).

Soil-biodegradable plastics (BDPs) have therefore emerged as a potential alternative to conventional plastic mulches. Because they are designed to biodegrade under soil conditions, BDP mulches can be incorporated into the soil after use, where they undergo abiotic deterioration and microbial degradation (8). Nevertheless, their incorporation introduces an exogenous organic carbon (C) source into the soil, with potential consequences for both soil physical structure and microbial functioning.

The presence of biodegradable and conventional plastic fragments may alter soil pore-size distribution, pore connectivity, and wettability, thereby affecting water infiltration, hydraulic conductivity, water-retention capacity, and gas transport (9, 10). These physical changes may, in turn, influence soil aggregation. Plastic fragments can directly interfere with contacts among mineral particles and aggregate-binding agents, while changes in pore architecture may modify oxygen diffusion and microbial activity, indirectly affecting aggregate formation and stability (11–13). Boots et al. (14), for example, observed a reduction in aggregates larger than 2000 µm and an increase in fractions between 250 and 63 µm following incubation with polylactic acid (PLA) and high-density polyethylene (HDPE) microplastics at 0.1% w/w. Similarly, in a two-year experiment, Zhao et al. (15) reported that both PLA and low-density polyethylene (LDPE) reduced the proportion of aggregates larger than 250 µm and increased the finer fractions, with more pronounced effects for PLA. However, the magnitude and direction of these responses depend on fragment concentration, size, shape, polymer composition, and soil properties (16).

The chemical composition and biodegradability of BDPs are particularly relevant because their decomposition may stimulate soil microorganisms. BDP concentrations of 1% w/w have been shown to increase microbial biomass and enzymatic activity (17). Several studies have also reported a prominent role of fungi in polymer degradation, although bacterial responses may vary according to polymer type and environmental conditions (18–21). Changes in the quantity and composition of the microbial community may affect soil aggregation because microbial biomass, fungal hyphae, extracellular polymeric substances, and microbial residues contribute to the binding of soil particles and the stabilization of aggregates.

Microbial utilization of BDP-derived C may also influence nitrogen (N) cycling. Because BDPs generally have a high C-to-N ratio, their degradation may promote microbial N immobilization to support biomass growth (17, 22). Consequently, BDP incorporation may modify the coupled cycling of C and N and their distribution among soil aggregate fractions. Soil aggregates are fundamental units of soil structure formed through interactions among mineral particles, organic matter, roots, and microorganisms (23). Their size distribution and stability regulate pore-network organization, substrate accessibility, microbial habitat conditions, nutrient transformations, and the physical protection of organic matter (23, 24). Microbial metabolites act as transient or persistent binding agents, whereas microbial residues, particularly fungal-derived compounds, may contribute to relatively stable C pools through association with clay minerals and organo-mineral matrices (25–27).

The stabilization of C and N within aggregates is also strongly controlled by soil physicochemical properties. Soil texture may regulate the interaction between BDP residues and the soil microbial community by controlling pore-size distribution, water and oxygen availability, and the interactions between microorganisms, organic substrates, and mineral surfaces (26, 28, 29). In fine-textured soils, the greater abundance and reactive surface area of clay and silt particles may enhance the retention of microbial products and residues and their physical and organo-mineral protection, whereas this stabilization capacity is generally lower in coarse-textured soils (25, 26). Consequently, soil texture may determine not only the magnitude of microbial responses to BDP incorporation but also the extent to which BDP-derived C and associated N are redistributed and stabilized within aggregate-associated pools (29).

Stable-isotope composition can provide additional information on the transformation and stabilization of C and N within aggregate fractions. Microbial assimilation and processing generally discriminate against heavier isotopes, whereas repeated microbial turnover and preferential losses of lighter isotopes may result in the relative enrichment of residual or microbially processed pools in ^{13}C and ^{15}N. Accordingly, finer soil fractions, which generally contain more extensively processed and mineral-associated organic matter, may exhibit higher $\delta^{13}C$ and $\delta^{15}N$ values than coarser fractions (30). Although, $\delta^{13}C$ and $\delta^{15}N$ values do not directly measure residence time or persistence, however, they can provide complementary information on the potential stabilization of C and N in the aggregate fractions after BDP addition.

The overall aim of this study was to determine how increasing concentrations of BDP fragments influence soil aggregate-size distribution and the allocation, microbial processing, and stabilization of C and N within aggregate fractions in soils differing in texture. Specifically, we hypothesized that: (i) BDP incorporation would alter aggregate-size distribution, with the magnitude and direction of the response depending on BDP concentration and soil texture; (ii) increasing BDP concentrations would increase microbial biomass carbon and bacterial and fungal target-gene abundance, with a stronger response of the fungal target, thereby promoting the incorporation of C and N into aggregate-associated pools; and (iii) enhanced microbial processing would produce progressively higher $\delta^{13}C$ and $\delta^{15}N$ values from coarse to fine aggregate fractions, with the strongest isotopic shifts occurring at the highest BDP concentrations and in soil providing greater physical and mineral protection of microbially processed organic matter.

TABLE 1 Main characteristics of the two soils considered. Source: Adapted from Mazzon et al. (17).

Main parameters	Loamy soil	Sandy soil
Sand (g kg_{ds}^{-1})	160	600
Loam (g kg_{ds}^{-1})	700	320
Clay (g kg_{ds}^{-1})	140	80
Soil reaction (pH in water)	6.65	7.63
Total organic C (g kg_{ds}^{-1})	22.8	18.0
Total N (g kg_{ds}^{-1})	2.2	2.0
Total carbonates ($CaCO_3$ %)	< 0.5	1.7

2 Materials and methods

2.1 Experimental setup

A laboratory experiment was carried out over one year on two different agricultural soils: a loamy soil (Cambisol; 31) and a sandy soil (Arenosol; 31), whose main characteristics are listed in Table 1. Briefly, after sieving at 2 mm and cleaning from plant debris, the soils were adjusted to 60% of their WHC (water holding capacity) and kept at 23 °C for a two weeks' pre-incubation. Afterwards, four treatments corresponding to three increasing doses of BDP and one control were prepared for each soil with the equivalent of 700 g of dry soil (17) distributed in plastic containers. Three replicates per treatment were prepared for a total of twelve samples for each soil).

The BDP used in the study is a commercial mulch film made of Mater-Bi® (grade EF04P), a biodegradable plastic material produced by Novamont S.p.A. The Mater-Bi® composition is based on modified starch and synthetic polymers (32) supplemented of carbon black (approximately 2.8%) to convert in from granules into film (17). The amount of BDP was added as small fragments (5-2mm) in three treatments equal to 100 (P100), 1, 000 (P1000) and 10, 000 (P10000) mg of BDP per kg of dry soil. The P100 treatment (100 mg kg^{-1} soil) corresponds to the mean annual quantity of BDP material incorporated into the soil (EN 17033 suggest 0.0063% = 63 mg kg^{-1} calculated on mean characteristics of BDP), while the P10000 treatment correspond to a loading rate of 1%, the quantity recommended in the EN 17033 to test biodegradability. The C content of BDP is equal to 60%, whereas no N is present in BDP chemical composition. Thus, the C added to soil with the different doses was 60 mg kg^{-1} (P100); 600 mg kg^{-1} (P1000) and 6000 mg kg^{-1} (P10000). The isotopic composition of BDP-derived C was equal to -25.1 $\delta^{13}C$ ‰ measured by CF-IRMS (continuous flow-isotope ratio mass spectrometry), with an elemental analyzer (Flash 2000, Thermo Fisher Scientific) coupled with an isotope ratio mass spectrometer (Delta V Advantage, Thermo Fisher Scientific), against the international standard V-PDB (Vienna-Pee Dee Belemnite). The BDP fragments were carefully mixed with the soil in containers covered with screw caps with few holes (of approximately 2 mm of diameter) to ensure the gas exchange during the incubation at 23 °C. The moisture of each container was weekly checked and restored, when necessary.

2.2 Microbial biomass carbon content

An aliquot of fresh soil samples, collected at the beginning of the experiment (T0), at month 6 (T1) and at the end of the experiment after one year (T2), was used for determining the microbial biomass carbon (C) content (MBC) following the procedure of Vance et al. (33). The C in the fumigated and non-fumigated extracts were determined using an elemental analyzer for liquid samples (TOC-VCPH/CPN).

2.3 DNA extraction from soil and quantitative PCR analysis

Soil samples for microbial investigations were collected from each experimental replicate at the beginning of the experiment (CK (T0)) prior to BDP addition, at month 6 (T1) and after a year (T2).

Each soil × treatment × time combination comprised three independent containers, representing the biological replicates. Immediately after collection, soil subsamples were stored at −80 °C. After completion of the experiment, all frozen samples were processed together, and one DNA extraction was performed per container and sampling time using the DNeasy PowerSoil Pro Kit (QIAGEN, Milan, Italy). Each DNA extract was subsequently analysed in three technical qPCR replicates for each target.

Total bacteria (Eubacteria) and total fungi were quantified using a QuantStudio™ 5 Real-Time PCR System (Applied Biosystems). Eubacteria were quantified using primers Eub338-F (5′-ACTCCTACGGGAGGCAGCAG-3′) and Eub518-R (5′-ATTACCGCGGCTGCTGG-3′), according to Baffoni et al. (34). Total fungi were quantified using primers NL1 (5′-GCATATCAATAAGCGGAGGAAAAG-3′) and NL4 (5′-CGGCGAGTGAAGCGGSAARAGCTC-3′), according to Vollmer et al. (35). qPCR reactions were performed in a final volume of 20 µL using PowerUp™ SYBR™ Green Master Mix (Applied Biosystems, Life Technologies), each primer at a final concentration of 200 nM, and 2 µL of 1:10-diluted DNA extract. Because DNA extracts were not normalized before amplification, no fixed DNA mass was used per reaction. Copy numbers were subsequently normalized according to the total amount of DNA recovered from each soil sample. Cycling conditions were 50 °C for 2 min and 95 °C for 2 min, followed by 40 cycles at 95 °C for 15 s, 60 °C for 15 s, and 72 °C for 60 s. Melt-curve analysis consisted of 95 °C for 15 s and 60 °C for 60 s, followed by a continuous increase to 95 °C at 0.15 °C s^{-1}. Melt curves were inspected to exclude primer-dimers and evident nonspecific amplification. The mean melting temperatures of the main amplification products were 84.61 °C for Eubacteria and 86.28 °C for total fungi. Standard curves were constructed separately for the bacterial and fungal assays using purified target-specific PCR products. Amplicons were serially diluted to obtain standards ranging from 10^4 to 10^8 gene copies per reaction. Amplification efficiencies were 101.34% for Eubacteria and 90.33% for total fungi, with R^2 values of 0.986 and 0.976, respectively. No-template controls were included in each qPCR run and showed no amplification. No formal inhibition test was performed; potential inhibition by soil-derived compounds was

minimized by diluting DNA extracts 1:10 before amplification. Formal analytical limits of detection and quantification were not independently determined. The lowest standard, corresponding to 10^4 gene copies per reaction, was therefore used as the operational quantification limit, and values below this threshold were reported as not detected (ND). Ct values were converted into gene copies per reaction using the corresponding standard-curve equation, Ct = m $\log_{10}$(N) + b, where m is the slope, b is the intercept, and N is the number of target copies. Thus, N was calculated as 10^((Ct – b)/m). The resulting copy numbers were normalized according to the total DNA recovered from each sample and the DNA amount contained in the qPCR aliquot. Final results were expressed as $\log_{10}$ target-gene copies per 100 mg of soil. When all three technical qPCR replicates of a DNA extract were below the operational detection threshold, the corresponding biological observation was recorded as ND. ND values were treated as missing, excluded from the statistical analyses, and were neither considered as zeros nor numerically substituted. Consequently, statistical analyses were performed using the available detected biological observations.

2.4 Soil aggregates fractionation and analyses

At the end of the one-year incubation period, the soil samples were subjected to a wet physical fractionation with two sieves, the first with a 250 µm mesh size and the second with a 50 µm mesh size, in order to recover three distinct soil aggregate fractions, as reported by Gioacchini et al. (36).

Briefly, an aliquot of 5 g of dry soil was evenly spread on the top of the first sieve, submerged in deionized water for a slaking time of 10 minutes, and then fractionated for 20 minutes by moving the sieves up and down for 50 times. The three aggregate fractions were quantitatively recovered. The macroaggregate fraction (2000-250 µm) was recovered from the top of the first sieve, the microaggregate fraction (250-50 µm) from the top of the second sieve, and the silt-clay fraction (< 50 µm) was collected at the bottom of the water container.

All the fractions were then dried at 60 °C, weighted and ground before being analysed for total organic carbon (C) and total nitrogen (N) concentration, and their isotopic ratios by an elemental analyser (EA, Flash 2000 Thermo Fisher Scientific) coupled with an isotopic ratio mass spectrometer (IRMS, Delta V Advantage Thermo Fisher Scientific). To ensure the accurate determination of organic carbon, the procedure recommends the pre-treatment of soil samples with few drops of HCl 6 M directly in silver capsules until the end of the effervescence. The samples are then dried at 80 °C on a heating plate (37) to eliminate possible interferences from inorganic carbon before the analysis with the elemental analyser. A separate aliquot of each sample was used for the determination of total N and its stable isotope composition without any pre-treatment.

The organic C content of the fractions (C_F) and the total N content of the fraction (N_F) were respectively determined as follows:

$$C_F(g_{C\ fraction} kg_{soil}^{-1}) = FW \times C$$

where FW is the fraction weight and C is the C concentration in the fraction.

$$N_F(g_{N\ fraction} kg_{soil}^{-1}) = FW \times N$$

where FW is the fraction weight and N is the N concentration in the fraction.

The C and N isotope composition were expressed as delta units (‰), for C:

$$\delta^{13}C(‰) = \left[\left(\frac{R_{sample}}{R_{std}}\right) - 1\right] \times 1000$$

where R_{sample} and $R_{standard}$ are the isotopic ratio $^{13}C/^{12}C$ of the sample and of the international Vienna-Pee Dee Belemnite carbonate standard (V-PDB), and for N:

$$\delta^{15}N(‰) = \left[\left(\frac{R_{sample}}{R_{std}}\right) - 1\right] \times 1000$$

where R_{sample} and $R_{standard}$ are the isotopic ratio $^{15}N/^{14}N$ of the sample and of the international standard which is the N_2 atmospheric gas.

2.5 Correction of aggregate weight for sand content

The two soils of the experiment were characterized by a significant difference in texture, particularly in their sand content. Therefore, to be able to compare the real effect of BDP addition on aggregates in the two soils, we determined the content of sand in each soil and its partitioning in the two fractions of macro and micro-aggregates. Specifically, 100 ml of 6% NaOCl at pH 8 was added to 10 g of dry soil and kept under stirring for 24 hours at room temperature. The samples were centrifuged (8000 rpm for 10 minutes) and the supernatant was discarded. 100 ml of 1M NaCl was added to the precipitate and stirred for 1 hour at room temperature, after centrifugation the supernatant was discarded, and 200 ml of deionized water was added and stirred for 24 hours. Finally, the samples were centrifuged, and the residue was collected in crucibles with deionized water, placed in an oven at 60 °C for one night and then weighed to determine the content of sand of each soil. Then, the dried samples were physically fractionated according to the procedure used for intact soil to determine the sand in the macroaggregate and microaggregate fractions. This value was used to correct the weight of the macro and microaggregates obtained from the fractionation of the intact soil, to express the weight of the macro and microaggregates on a sand-free basis and make possible the comparison between the two soils without the interference of the sand.

2.6 Data handling and statistical analysis

Statistical analyses were performed using the R environment (38). Two complementary statistical approaches were adopted according to the distribution of the data and the structure of the experimental design.

Microbial biomass carbon (MBC) was analyzed using a repeated-measures design in which treatment was specified as a between-subject factor and time as a within-subject factor. Replicate identity nested within treatment was used as the experimental subject, and treatment, time, and treatment × time effects were tested. Because T0 measurements were available only for the control, the factorial analysis included T1 and T2 only. Microbial abundance data were analyzed using generalized estimating equations (GEE) to account for repeated measurements over time. Treatment, time, and their interaction were included as fixed effects, while replicate identity was used as the clustering variable with an exchangeable working correlation structure. Analyses of treatment effects were restricted to T1 and T2 because all treatments were represented at these time points. GEE models were fitted using all available quantifiable observations after exclusion of ND values. Container identity, rather than the individual technical qPCR measurement, defined the biological cluster. Therefore, when only one quantifiable biological replicate remained within a soil × treatment × time combination, that condition contributed one biological cluster to the global model; technical qPCR replicates did not increase the biological sample size. Model-based contrasts involving such sparsely represented combinations were interpreted cautiously. When significant interactions were detected, simple-effects comparisons were performed with adjustment for multiple testing with adjusted pairwise comparisons (Holm/Tukey), and the "emmeans" test was applied.

For both MBC and microbial abundance data, control samples were additionally analyzed across T0, T1, and T2 using a separate repeated-measures model.

Aggregate-associated C, N, C:N, and stable isotope data were analyzed using a repeated-measures factorial design, with soil type and treatment as between-subject factors and aggregate fraction (macroaggregate, microaggregate and silt–clay) as a within-subject factor. Individual experimental replicates (soil × treatment × replicate) were specified as subjects to account for the non-independence of fractions obtained from the same soil sample. Greenhouse–Geisser-adjusted degrees of freedom were used for within-subject effects where appropriate. Significant interactions were followed by estimated marginal means and multiplicity-adjusted pairwise comparisons. Because two $\delta^{13}C$ observations were missing, $\delta^{13}C$ was additionally evaluated using a linear mixed-effects model with replicate identity as a random intercept, allowing incomplete repeated observations to be retained.

Aggregate fraction mass was converted to relative mass proportions and analyzed as three-part compositional data after isometric log-ratio transformation; effects of soil type, treatment and their interaction were assessed by multivariate analysis of variance using Pillai's trace.

Marginal comparisons among aggregate fractions within each soil type were evaluated from the repeated-measures model using estimated marginal means (EMMs). Aggregate fraction was treated as a within-subject factor, whereas soil type and treatment were included as between-subject fixed factors, with each experimental replicate defined as the repeated-measures subject. Pairwise contrasts among fractions were then performed within each soil type, and p-values were adjusted for multiple comparisons using the Holm procedure. In general, differences were considered statistically significant at p-values < 0.05.

3 Results

3.1 Microbial biomass carbon

After six months of incubation, MBC showed a similar response pattern in the two soils, although absolute values differed markedly (Figures 1A, B). At T1, P100 and P1000 did not differ significantly from CK, whereas P10000 produced a marked increase in MBC in both soils, reaching approximately 238 mg kg_{ds}^{-1} in the sandy soil

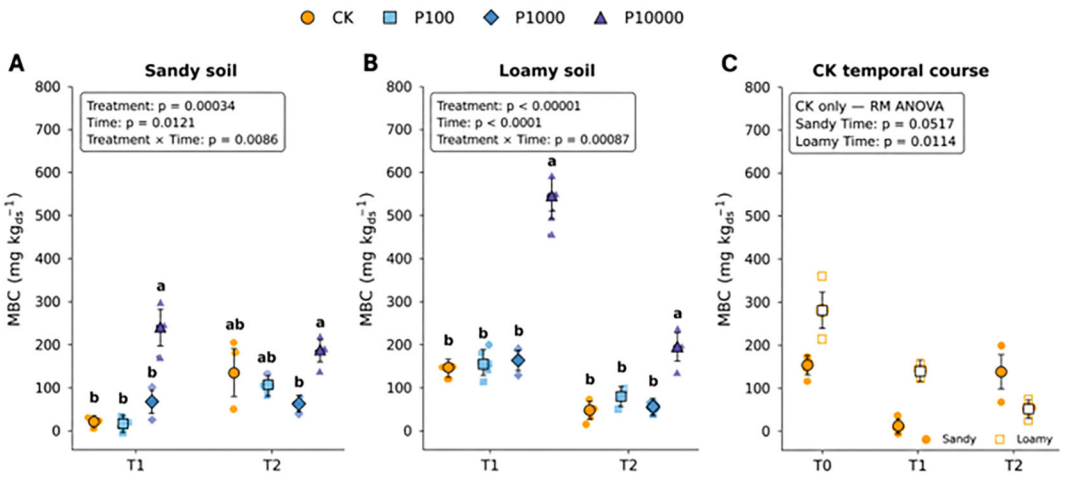

FIGURE 1
Microbial biomass carbon (MBC) in sandy **(A)** and loamy **(B)** soils at T1 and T2. Individual observations are shown together with mean ± SE. Different lowercase letters indicate significant differences among treatments within each sampling time based on multiplicity-adjusted *post hoc* comparisons. Temporal evolution of the control was analysed separately **(C)** across T0, T1 and T2 using a CK-only repeated-measures ANOVA. Corresponding p-values are reported within each panel.

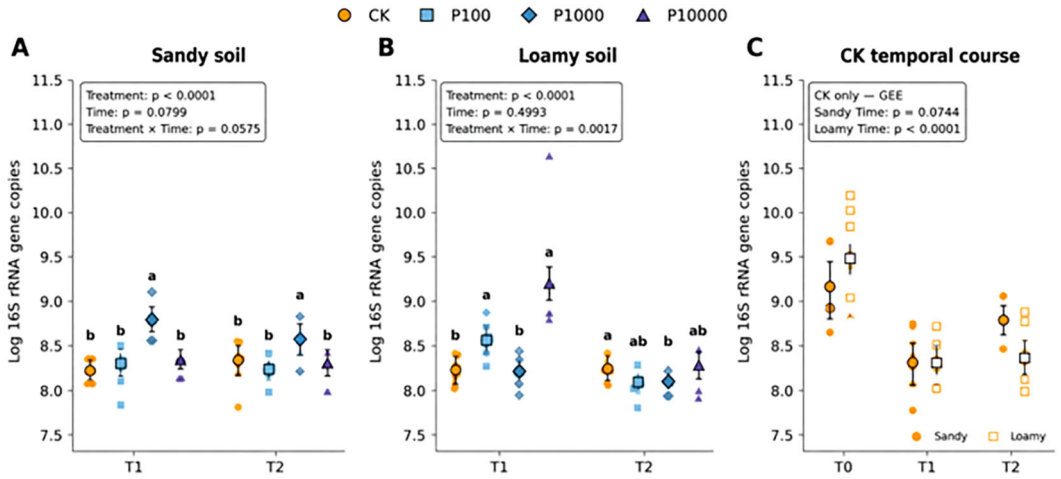

FIGURE 2
Bacterial abundance, expressed as log-transformed 16S rRNA gene copies, in sandy **(A)** and loamy **(B)** soils at T1 and T2. Individual observations are shown together with mean ± SE. Different lowercase letters indicate significant differences among treatments according to multiplicity-adjusted *post hoc* comparisons. Temporal evolution of the control was analysed separately **(C)** across T0, T1 and T2 using a CK-only GEE model. Corresponding p-values are reported within each panel.

and 583 mg kg_{ds}^{-1} in the loamy soil. A significant Treatment × Time interaction was detected in both sandy ($p = 0.0086$) and loamy soils ($p = 0.00087$), indicating that treatment effects changed over time. In sandy soil, at T2, MBC increased in CK and P100 but remained stable or tended to decrease with P1000 and P10000. However, P10000 remained the highest treatment significantly higher than P1000 and about 25% higher than CK. In loamy soil a decrease in MBC was observed in CK and all the treatments, with the greatest reduction found with P10000. Despite this trend, however, MBC in this treatment remained significantly higher than CK, P100 and P1000. The CK temporal course analyzed separately across T0, T1 and T2 showed a significant time effect in the loamy soil ($p = 0.0114$) where MBC decreased from the beginning to the end of the experiment, whereas the temporal effect in the sandy soil did not reach significance ($p = 0.0517$).

3.2 Bacterial and fungal target-gene abundance

Bacterial 16S rRNA gene-copy abundance was significantly affected by treatment in both soils, although the temporal response differed between sandy and loamy soils (Figure 2). In sandy soil, Treatment was significant ($p < 0.0001$), whereas neither Time ($p = 0.0799$) nor the Treatment × Time interaction ($p = 0.0575$) reached statistical significance. Consequently, treatment differences were interpreted marginally across T1 and T2. P1000 showed the highest bacterial 16S rRNA gene-copy abundance and was significantly higher than CK, P100 and P10000, while the latter treatments did not differ significantly from one another. In loamy soil, a significant Treatment × Time interaction was detected ($p = 0.0017$). At T1, P100 and P10000 showed significantly higher bacterial 16S rRNA gene-copy abundance than CK and P1000. At T2, treatment differences were less pronounced, with P1000 significantly lower than CK, while P100 and P10000 showed intermediate values. The CK-only temporal analysis indicated a significant effect of time in the loamy soil ($p < 0.0001$) where the bacterial 16S rRNA gene-copy abundance significantly decreased after six months of incubation (T1), whereas no significant temporal effect was detected in the sandy soil ($p = 0.0744$).

Fungal target-gene abundance (Figure 3) was significantly affected by both treatment and time in sandy soil (both $p < 0.0001$), whereas the Treatment × Time interaction was not significant ($p = 0.3111$) (Figure 3A). Therefore, treatment effects were interpreted marginally across T1 and T2. P1000 showed the highest fungal target-gene abundance, CK the lowest, while P100 and P10000 showed intermediate responses. Fungal target-gene abundance increased significantly with time across treatments. In loamy soil, Treatment, Time and their interaction were all significant ($p < 0.0001$). At T1, P10000 showed the highest fungal target-gene abundance, P100 was intermediate, whereas CK and P1000 showed the lowest values. At T2, CK and P10000 showed the highest target-gene abundance, P100 was lower, and P1000 exhibited the lowest values. The separate CK temporal analysis showed a significant effect of time in both sandy and loamy soils with a decrease from the beginning to T1 and a further increase from T1 to T2 ($p < 0.0001$).

3.3 Fraction weight

The mass recovery after the fractionation procedure ranged between approximately 97 and 99% of the initial soil mass (Supplementary Table S2). The amount of sand and its distribution between macroaggregates and microaggregates was different in the two soils. In the loamy soil the sand accounted for 33% of the weight of macroaggregates and almost 38% of microaggregates. In the sandy soil, on the contrary, the sand accounted for 90% in the macroaggregates and almost 74% in the microaggregates (Supplementary Table S2). The sand corrected weight of the aggregate fractions (FW) for the two soils, after one year of incubation, is reported in Table 2. Macroaggregates and microaggregates, both showed significant differences between the soil type with the highest value in the loamy soil (+78% for

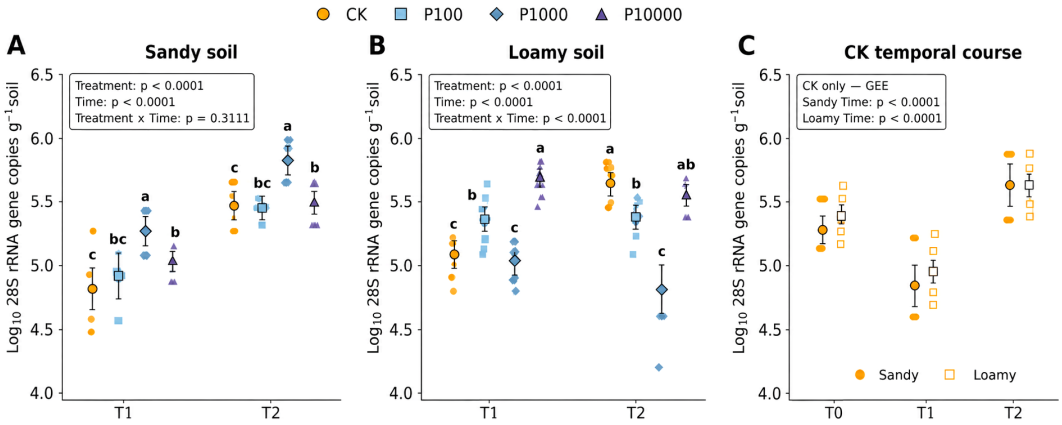

FIGURE 3
Fungal abundance, expressed as log-transformed 28S rRNA gene copies in sandy **(A)** and loamy **(B)** soils at T1 and T2. Individual observations are shown together with mean ± SE. Different lowercase letters indicate significant differences among treatments according to multiplicity-adjusted *post hoc* comparisons. Temporal evolution of the control was evaluated separately **(C)** across T0, T1 and T2 using a CK-only GEE model. Corresponding p-values are reported within each panel.

TABLE 2 **Mean ± standard deviation of fraction-associated soil parameters in the Loamy and Sandy soils: fraction weigh (FW), C content of the fractions (C_F), N content of the fractions (N_F), C-to-N ratio (CN), stable C isotope ($\delta^{13}C$), and stable N isotope ($\delta^{15}N$).**

Parameter	Loamy soil	Sandy soil	*p-value*
FW (g kg_{ds}^{-1})			
Macroaggregates	237 ± 39	51 ± 3	*< 0.001*
Microaggregates	315 ± 23	90 ± 6	*< 0.001*
Silt & Clay	116 ± 57	124 ± 33	*0.204*
C_F ($g_{C\ fraction}$ kg_{ds}^{-1})			
Macroaggregates	6.15 ± 1.29	5.56 ± 1.64	*0.225*
Microaggregates	9.01 ± 0.81	8.08 ± 1.22	*0.065*
Silt & Clay	1.93 ± 1.00	4.43 ± 1.17	*< 0.001*
N_F ($g_{N\ fraction}$ kg_{ds}^{-1})			
Macroaggregates	0.622 ± 0.125	0.467 ± 0.119	*0.007*
Microaggregates	0.952 ± 0.084	0.759 ± 0.125	*< 0.001*
Silt & Clay	0.227 ± 0.113	0.474 ± 0.124	*< 0.001*
CN			
Macroaggregates	9.9 ± 0.3	12.0 ± 2.4	*0.038*
Microaggregates	9.5 ± 0.5	10.7 ± 0.4	*< 0.001*
Silt & Clay	8.5 ± 0.3	9.4 ± 0.1	*< 0.001*
$\delta^{13}C$ (‰)			
Macroaggregates	-25.6 ± 0.1	-25.0 ± 0.4	*< 0.001*
Microaggregates	-25.6 ± 0.2	-25.3 ± 0.4	*< 0.001*
Silt & Clay	-25.4 ± 0.1	-25.5 ± 0.0	*0.009*
$\delta^{15}N$ (‰)			
Macroaggregates	5.56 ± 0.13	5.43 ± 1.00	*0.686*
Microaggregates	5.74 ± 0.12	7.71 ± 0.34	*< 0.001*
Silt & Clay	5.94 ± 0.37	8.59 ± 0.26	*< 0.001*

Descriptive comparisons between soil types within each aggregate fraction were assessed using the Kruskal–Wallis test; p-values < 0.05 are shown in italics.

macroaggregates and +71% for microaggregates), while the silt- clay fraction was similar in the two soils (Table 2).

Because macroaggregates, microaggregates and the silt–clay fraction represents compositional components of the same soil sample, their relative distribution was analyzed using an isometric log-ratio transformation followed by MANOVA. Aggregate composition was statistically significantly affected by soil type, BDP treatment and their interaction (all $p \leq 0.0022$; Table 3).

In the loamy soil, on average, the microaggregate fraction was higher than macroaggregates and silt- clay that did not differ between them (Table 3). The CK was characterized by approximately 28.8% macroaggregates, 42.7% microaggregates and 28.5% silt–clay. P100 and P1000 increased the relative proportion of microaggregates to about 50%, whereas P10000 markedly increased macroaggregates to 45.3% and reduced the silt–clay fraction to 8.9%. In the sandy soil, the aggregates composition was different from that of the loamy, in this soil the highest relative FW was that of the silt and clay, than the microaggregates and the macroaggregates (Table 3). The CK consisted of 17.1% macroaggregates, 31.4% microaggregates and 51.5% silt–clay. In this soil P10000 aggregate composition towards larger fractions, increasing macroaggregates to 24.7% and microaggregates to 41.5%, while decreasing the silt–clay fraction to 33.8%. The other two BDP doses, on the contrary, did not show a clear effect on the aggregate relative distribution.

3.4 C and N content of the aggregate fractions

In both soils, C and N content (C_F and N_F, respectively) differed among aggregate fractions. Marginal comparisons showed that the highest C_F and N_F contents were generally associated with microaggregates, whereas the silt–clay fraction contained the lowest amounts (Figures 4, 5). Carbon content of macro- and microaggregates did not differ significantly between soils, whereas C_F associated with the silt–clay fraction was statistically significantly higher in sandy soil. In contrast, N_F associated with macro- and

TABLE 3 Relative aggregate fraction mass (%) in the two soils (mean ± SD).

Parameter	Loamy soil			Sandy soil		
	Macro aggregates	Micro aggregates	Silt & Clay	Macro aggregates	Micro aggregates	Silt & Clay
Relative FW (%)	**35.6 ± 6.6^{B}**	**47.3 ± 4.0^{A}**	**17.1 ± 7.9^{C}**	**19.5 ± 3.4^{C}**	**34.5 ± 5.2^{B}**	**46.0 ± 8.2^{A}**
CK	28.8 ± 3.6^{b}	42.7 ± 4.3^{b}	28.5 ± 6.3^{a}	17.1 ± 0.5^{b}	31.4 ± 4.6^{b}	51.5 ± 5.0^{a}
P100	34.0 ± 1.7^{b}	50.5 ± 0.8^{a}	15.5 ± 0.9^{b}	17.7 ± 2.0^{b}	32.4 ± 1.8^{b}	49.9 ± 3.2^{a}
P1000	34.2 ± 0.9^{b}	50.1 ± 0.9^{a}	15.7 ± 1.2^{b}	18.4 ± 1.0^{b}	32.6 ± 4.2^{ab}	48.9 ± 4.9^{a}
P10000	45.3 ± 2.6^{a}	45.8 ± 2.4^{ab}	8.9 ± 0.2^{b}	24.7 ± 1.6^{a}	41.5 ± 2.3^{a}	33.8 ± 3.1^{b}
Treatment p-value	*< 0.001*	*0.016*	*< 0.001*	*< 0.001*	*0.022*	*0.003*

Primary inference used ILR-MANOVA (Pillai: Soil, $p < 0.0001$; Treatment, $p < 0.0001$; Soil × Treatment, $p = 0.0022$). Uppercase letters denote Holm-adjusted marginal fraction differences within soil; lowercase letters denote Tukey-adjusted treatment differences within the same soil fraction ($p < 0.05$).
In bold are reported mean ± SD in the aggregate fractions averaged for the BDP dose.

microaggregates was higher in loamy soil, while the silt–clay fraction contained more N in sandy soil (Table 2). The C:N ratio was higher in sandy than in loamy soil. Marginal fraction comparisons indicated a decrease in C:N ratio towards the finer aggregate fractions, in both soils (Figures 4, 5).

In loamy soil, the highest C_F and N_F content in macroaggregates was measured with P10000. The opposite was found in the silt-clay fraction where C_F showed a dose-dependent decline with P100 and P1000 statistically lower than CK and P10000 that showed the lowest C_F value. Looking at N_F content, BDP treatments reduced N_F relative to CK. In microaggregates, C_F showed a significant treatment response, with P10000 higher than CK and P100 and P1000 showing intermediate values, whereas no significant treatment effect was detected for N_F (Figure 4).

In sandy soil, treatment effects were also fraction dependent. For C_F, P10000 increased the macroaggregate-associated C_F relative to CK and produced the highest value in microaggregates, while the other two doses showed intermediate values between P10000 and CK. In the silt–clay fraction, C_F progressively decreased with increasing BDP dose. For N_F, no significant treatment differences were detected in macro- or microaggregates, whereas P10000 significantly reduced N_F in the silt–clay fraction compared with CK, P100 and P1000 (Figure 5).

3.5 $\delta^{13}C$ and $\delta^{15}N$ of the aggregates

The $\delta^{13}C$ composition differed among aggregate fractions in both soils. In loamy soil, macroaggregates and microaggregates showed comparable $\delta^{13}C$ values, whereas the silt–clay fraction was enriched in ^{13}C, showing less negative values. In sandy soil, the opposite pattern was observed with a depletion of ^{13}C in the following order: macroaggregates to microaggregates and silt–clay fraction characterized by the most negative values. Marginal treatment comparisons across fractions did not reveal significant effects of BDP dose on $\delta^{13}C$ in either soil (Table 4).

The $\delta^{15}N$ composition showed a progressive enrichment towards finer fractions. In loamy soil, macroaggregates showed lower $\delta^{15}N$ than microaggregates and the silt–clay fraction, whereas the latter two fractions did not differ significantly. In sandy soil, the shift in $\delta^{15}N$ from macroaggregates to microaggregates and further to the silt–clay fraction was particularly pronounced. Accordingly, $\delta^{15}N$ values differed between soils in the microaggregate and silt–clay fractions, but not in macroaggregates (Table 2). No significant marginal treatment effect was detected in loamy soil. In sandy soil, BDP dose affected $\delta^{15}N$ when averaged across fractions, with P10000 showing higher values than P1000, whereas CK and P100 showed intermediate values (Table 4).

4 Discussion

4.1 Influence of BDP on microbial biomass and target-gene abundance

Unlike conventional plastics, BDPs constitute not only a physical input to the soil but also a biochemical one, as the carbon embedded in their structure can be utilized by the microbial community for growth and metabolic activity (39–41). In this study, we added increasing amounts of C with the different doses, 60 mg kg^{-1} (P100), 600 mg kg^{-1} (P1000) and 6000 mg kg^{-1} of soil (P10000), but after six months a stimulation of the microbial biomass (MBC) growth was observed only with the highest BDP dose (1% - P10000) in both soils. We cannot exclude, however, that the other two treatments, particularly P1000, might have influenced the microbial biomass in the first period of incubation that was not detectable anymore after six months. Other studies have demonstrated that the effect of plastic to the growth and activity of microorganisms is stronger soon after their addition to the soil and then declines (42, 43), therefore is probable that a six-month period would be too long to measure changes in the MBC with the lower doses of BDP. On the other hand, in a study carried out by 41 with biodegradable plastics added to a sandy and loamy soil at 0.1 and 1% (w/w), the lower dose, did not induce any increase in MBC after 4 weeks of incubation. Lower doses of BDP mean lower amount of exogenous C added to the soil but also reduced physical modification of the soil structure, with small changes in terms of porosity and consequent O_2 diffusion and therefore a reduced effect on the microbial biomass. After one year of incubation, although MBC values declined, the P10000 treatment still showed higher values than both the CK and the other BDP treatments, meaning that the effect of this huge amount of C added on the microbial

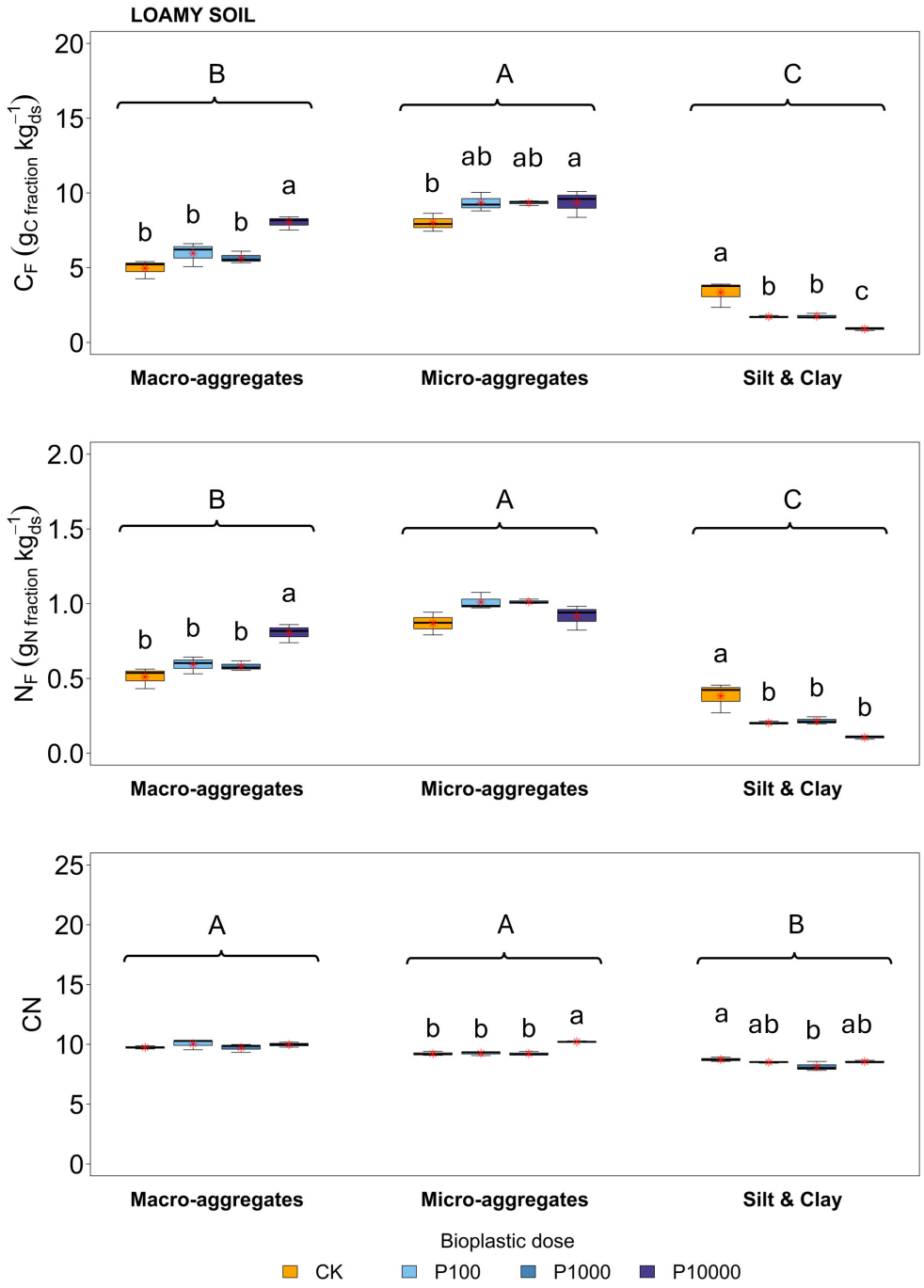

FIGURE 4
Marginal comparison among fractions of organic C (C_F) and N (N_F) content of the fractions and C to N ratio (CN) in the Loamy soil. Black line in the boxplot indicate the median and the black dots the average Different uppercase letters indicate significant marginal differences among aggregate fractions, while different lowercase letters indicate significant differences among treatments within the same aggregate fraction, based on estimated marginal means derived from the repeated-measures ANOVA and multiplicity-adjusted *post hoc* comparisons using the Holm procedure ($p < 0.05$).

biomass may persist for long time. Moreover, during the incubation, not only BDP residues, but also the by-products generated during their degradation may support the growth of the MBC and possibly induce shifts in microbial community composition (44–46) In the two soils with distinct physicochemical properties the microbial community response to BDP doses was partly different. In sandy soil, P1000 produced the highest marginal bacterial and fungal abundance across the two sampling times, whereas in loamy soil treatment responses were strongly time dependent. In loamy soil, the strongest microbial responses were observed at T1: P10000 produced the highest fungal abundance, whereas bacterial 16S rRNA gene-copy abundance was similarly elevated under P100 and P10000. This evidence partly contradicts our hypothesis that the fungal community would be more stimulated by the addition of the highest dose of BDP. A soil-type specific variation in bacterial and fungal abundance, was also reported in Bandopadhyay et al. (47) after two years of repeated tillage of biodegradable mulch into two soils with texture similar to our soils. The authors found an

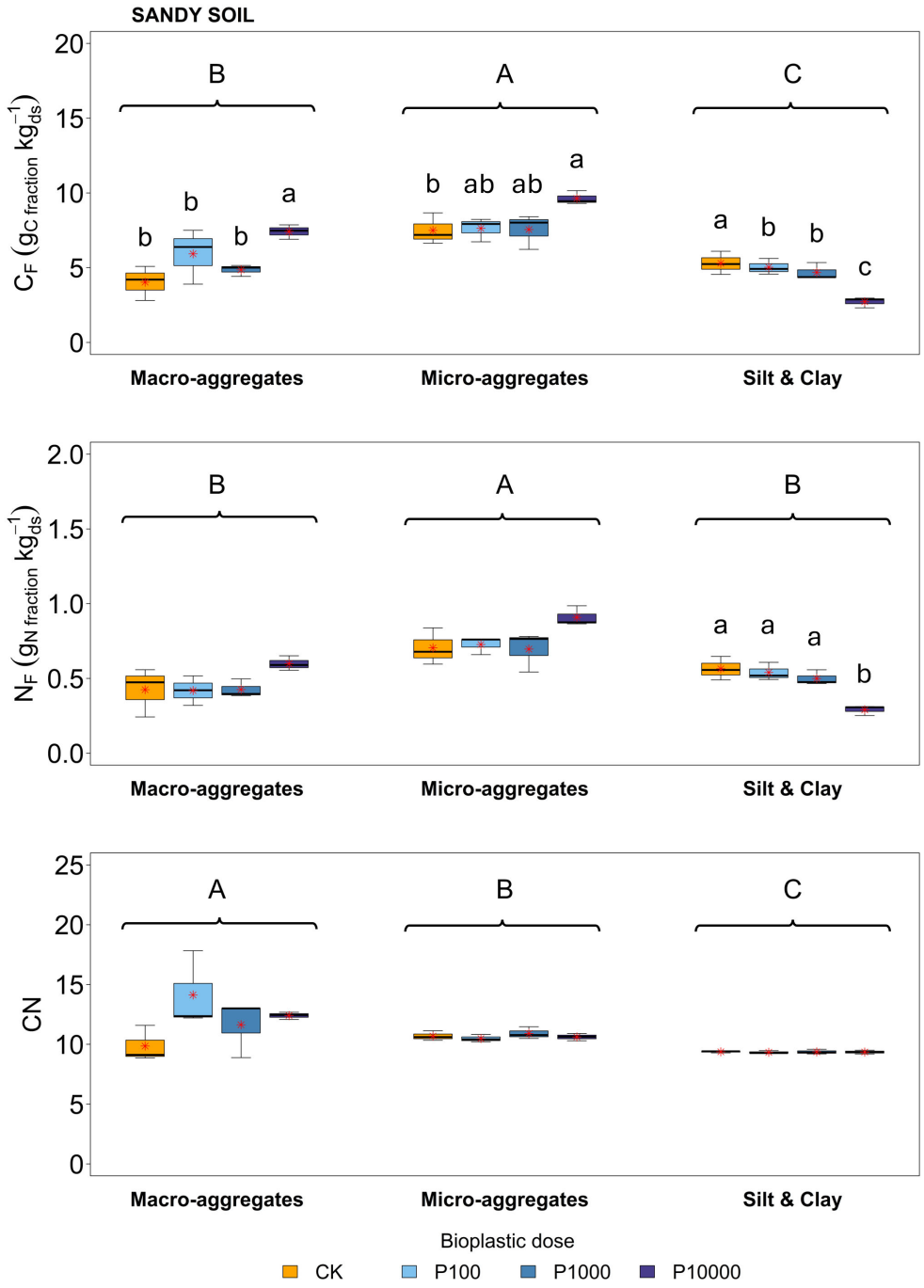

FIGURE 5
Marginal comparison among fractions of organic C (C_F) and N (N_F) content of the fractions and C to N ratio (CN) in the Sandy soil. Black line in the boxplot indicate the median and the black dots the average Different uppercase letters indicate significant marginal differences among aggregate fractions, while different lowercase letters indicate significant differences among treatments within the same aggregate fraction, based on estimated marginal means derived from the repeated-measures ANOVA and multiplicity-adjusted *post hoc* comparisons using the Holm procedure ($p < 0.05$).

increase of both bacteria and fungi in the silty soil, and only of bacteria in the sandy soil. Our results partly differed since we found an increase in fungal target-gene abundance also in the sandy soil although not with the highest BDP dose. The different response of the bacterial and fungal abundance to the BDP dose in the two soils was quite unexpected but it is possibly related to the impact of the doses on soil respiration and CO_2 losses that we measured in a previous study at the beginning of the incubation of the two soils (17). In that study, P10000 in the sandy soil has induced an extremely high increase in CO_2 emissions compared to P1000 and P100 and compared to the loamy soil. Indeed, we could not distinguish the source of the released CO_2, if derived from BDP as effect of degradation or from soil because of an effect of priming, but we can hypothesize that, in spite of the source, most of the available C has been lost as CO_2 rather than being metabolized by microorganisms. On the contrary, P1000, by supplying less fragments and C

TABLE 4 Carbon and nitrogen stable isotope composition ($\delta^{13}C$ and $\delta^{15}N$; ‰) in the two soils (mean ± SD).

Parameter	Loamy soil				Sandy soil			
	Macro aggregates	Micro aggregates	Silt & Clay	TMM	Macro aggregates	Micro aggregates	Silt & Clay	TMM
$\delta^{13}C$ (‰)	-25.57 ± 0.11^{B}	-25.61 ± 0.25^{B}	-25.38 ± 0.12^{A}		-25.03 ± 0.39^{A}	-25.28 ± 0.37^{AB}	-25.50 ± 0.04^{B}	
CK	-25.66 ± 0.10	-25.64 ± 0.03	-25.56 ± 0.07	**-25.62 ± 0.03**	-25.12 ± 0.50	-25.41 ± 0.09	-25.50 ± 0.04	**-25.34 ± 0.14**
P100	-25.45 ± 0.10	-25.82 ± 0.48	-25.36 ± 0.03	**-25.54 ± 0.13**	-24.76 ± 0.50	-25.39 ± 0.09	-25.55 ± 0.05	**-25.23 ± 0.14**
P1000	-25.60 ± 0.08	-25.49 ± 0.05	-25.31 ± 0.05	**-25.47 ± 0.03**	-25.08 ± 0.20	-24.96 ± 0.72	-25.48 ± 0.04	**-25.21 ± 0.23**
P10000	-25.56 ± 0.01	-25.50 ± 0.04	-25.30 ± 0.06	**-25.45 ± 0.02**	-25.26 ± 0.03	-25.36 ± 0.09	-25.49 ± 0.02	**-25.38 ± 0.01**
$\delta^{15}N$ (‰)	5.56 ± 0.13^{B}	5.74 ± 0.12^{A}	5.94 ± 0.37^{A}		5.43 ± 1.00^{C}	7.71 ± 0.34^{B}	8.59 ± 0.26^{A}	
CK	5.53 ± 0.06	5.65 ± 0.09	5.84 ± 0.08	**5.68 ± 0.03**	5.14 ± 0.97	7.71 ± 0.14	8.77 ± 0.07	**7.21 ± 0.33^{ab}**
P100	5.45 ± 0.13	5.80 ± 0.16	6.21 ± 0.19	**5.82 ± 0.15**	5.39 ± 0.76	7.60 ± 0.15	8.32 ± 0.06	**7.10 ± 0.28^{ab}**
P1000	5.61 ± 0.18	5.83 ± 0.00	5.80 ± 0.38	**5.75 ± 0.08**	4.61 ± 0.90	7.38 ± 0.30	8.43 ± 0.20	**6.80 ± 0.45^{b}**
P10000	5.64 ± 0.04	5.65 ± 0.08	5.90 ± 0.63	**5.73 ± 0.19**	6.59 ± 0.19	8.16 ± 0.15	8.83 ± 0.19	**7.86 ± 0.16^{a}**

Uppercase letters indicate Holm-adjusted marginal differences among aggregate fractions within each soil type. The "Treatment marginal mean" columns (TMM) report replicate-level treatment means averaged across fractions (mean ± SD); different lowercase letters indicate Tukey-adjusted marginal treatment differences within the same soil type ($p < 0.05$).
In bold are reported mean ± SD in the aggregate fractions averaged for the BDP dose.

may have reduced the initial CO_2 losses and was associated with higher bacterial and fungal target-gene abundance.

In both soils, however, the main changes in bacterial and fungal abundance were observed after six months of incubation, while few differences were observed after one year only for fungi. This increase in fungal target-gene abundance is consistent with previous studies reporting increases in fungi -and, to a lesser extent, bacteria- following BDP addition (44, 47–49). In general, these findings are explained by the enhanced availability of C released during polymer degradation, which, although not representing a major C source in soils, can nonetheless influence microbial community composition, abundance, and activity (44, 47, 48). The higher fungal target-gene abundance may be related to their superior capacity to decompose polymers (49). Fungi are indeed recognized as key colonizers and degraders of BDPs due to their ability to produce cutinases, enzymes that accelerate BDP degradation and carbon release into the soil (47).

4.2 Influence of BDP on soil aggregation

Following one year of incubation, BDPs affected the distribution of soil aggregates and the associated carbon and nitrogen contents in both soils, with additional variations attributable to soil type. The increase of macroaggregates abundance was enhanced in both soils treated with the highest BDP dose, whereas the silt-clay fraction decreased. Conversely, the lower BDP doses mainly affected the microaggregate fraction in the loamy soil, whereas in the sandy soil shifts in aggregate composition were restricted to P10000. A different response of the two soils in terms of aggregation was expected, as different soil characteristics such as clay content and soil biochemical properties have been identified as key determinants of aggregate formation (50, 51). In a sandy loam soil, for example, De Souza MacHado et al. (52) observed that plastic fragments with size and shape similar to those of soil mineral particles exerted a generally weaker influence on aggregation. This agrees with the weak effect of BDP on aggregation in the sandy soil where only the highest dose was able to favor an increase in the recovery of macro- and micro-aggregate fractions.

Moreover, the influence of BDP fragments on aggregate abundance has been shown to vary according to the amount, size, and shape of the fragments (16, 33). For instance, PLA and HDPE particles sized 65-103 µm, added at 0.1% w/w, reduced macroaggregates and increased microaggregates (14). We observed a similar behaviour in the loamy soil where the P1000 and P100 treatments lead to an increase of microaggregates recover but not of macroaggregates.

Increasing amount of BDP fragments can influence the abundance of the aggregate fractions by changing soil porosity and the oxygen diffusivity, thereby modifying oxygen availability for microorganisms (12) and affecting numerous microbially mediated processes, including aggregate formation. However, most importantly, increasing doses of BDP mean increasing C input to soil that can be used by the microbial community for its growth and activity (39, 41, 53).

In this study, a stimulation of microbial biomass carbon (MBC) was observed at the highest BDP dose (1% - P10000) in both soils.

Such high amount of exogenous C may have supported the turnover of microorganisms, both bacteria and fungi, whose residues and metabolic by-products could contribute to the increase in macroaggregates abundance and in their associated C and N. Furthermore, BDP fragments may have acted directly as nuclei for macroaggregate once embedded within soil aggregates together with soil mineral (primary soil particles and microaggregates) and organic (soil organic matter and microbial biomass) components, thereby promoting macroaggregate formation as well as the accumulation and turnover of associated C and N (51, 54). However, since residual BDP fragments potentially embedded in the aggregate fractions were not quantified, some of the measured aggregate-associated C may also represent residual BDP-derived material rather than stabilized native soil C. The observed enhancement in aggregation recovery was also accompanied by the occlusion of part of the silt-clay fraction within the larger aggregates and a

concomitant reduction in its free portion (55). Consequently, changes in the relative distribution of aggregate size classes influenced the C and N associated, which increased in macroaggregates (and in microaggregates in the sandy soil) and decreased in the free silt–clay fraction. This rearrangement of the three aggregates size classes with the occlusion of finest fractions in the macroaggregates, caused by the highest BDP dose, may contribute to preserving C and N from microbial attack and mineralization, according to the model proposed by Six et al. (56).

If the effect of P10000 on the aggregates size distribution was similar in the two soils and responded to our hypothesis with the expected increase in macroaggregates abundance, the impact of the other doses was much lower and not able to influence the recovery of macroaggregates. In the sandy soil, the lower BDP doses did not affect the aggregation but only the amount of C and N associated to the silt-clay fraction that progressively decreased with the increasing of the dose. In the loamy soil, on the contrary, P100 and P1000 caused an increase of microaggregates abundance and of their C and N content and a significant decrease of the silt-clay and their associated C and N. The lower doses of BDP have provided less fragments and less C to microorganisms compared to P10000, and this may have limited the macroaggregates abundance. We cannot exclude, however, that the higher amounts of free microaggregates would result from a faster turnover of macroaggregates formed in earlier incubation period, which breakdown has freed some of the microaggregates previously occluded inside the macroaggregates (55). Importantly, within microaggregates, organic C and N are protected from decomposition due to physical constraints that limit oxygen diffusion and enzyme accessibility (57, 58); as a result, this fraction plays a central role in the long-term protection of soil C and N.

In both soils, the decrease in the C:N ratio along the aggregate size gradient from macroaggregates to silt-clay fractions would reflect the predominantly microbial origin of organic compounds associated with the silt-clay fraction, which is typically enriched in N relative to the original substrates processed by microorganisms (58–60). Carbon and N in this fraction are considered the most stable in soil (61, 62) since they are linked to mineral components through chemical interaction and stabilized through persistent binding agents (63).

In addition to the C:N ratio, the isotopic composition of C and N provides insights into the origin, transformation, and potential stabilization of organic matter within aggregate fractions (64). $\delta^{15}N$ values increased from macroaggregates to silt-clay in both soils, although the shift was more pronounced in the sandy soil. Unexpectedly, in the sandy soil, $\delta^{13}C$ did not follow the same pattern and instead showed a depletion from macroaggregates to the silt-clay fraction. In the loamy soil, macro and microaggregates exhibited similar $\delta^{13}C$ values, whereas silt-clay fraction was enriched in ^{13}C.

These differences suggest that the rates of transformation and stabilization processes of organic C and N diverge between the two soils, largely as result of their contrasting textures. Among the overall soil properties, the heavier texture of the loamy soil may have promoted the greater abundance of macro and microaggregates in which organic C and N are protected from degradation. This finding is consistent with the observed increase in microbial biomass carbon and bacterial and fungal target-gene abundance. Therefore, the increase in both $\delta^{13}C$ and $\delta^{15}N$ values in the smaller fractions supports the interpretation that C and N were associated and protected in these aggregate classes after microbial recycling and transformation (30).

Conversely, the high sand content of the sandy soil could have created conditions more conducive to high mineralization rates and CO_2 losses (17). In this context, the $\delta^{13}C$ trend may reflect a rapid mineralization dynamics and the preferential microbial utilization of labile, ^{13}C-enriched compounds, with the consequent stabilization of more recalcitrant, ^{13}C-depleted molecules in the silt–clay fraction (30). The increase in $\delta^{15}N$ values from macroaggregates to microaggregates and silt-clay fraction may also indicate a combined effect of rapid mineralization-immobilization turnover and subsequent stabilization of N highly recycled and fractionated within the microaggregates and silt-clay fraction. Although $\delta^{13}C$ differed among aggregate fractions, the analysis did not detect a significant marginal effect of BDP treatment in either soil. The isotopic differences appear to reflect primarily soil-specific C transformation and stabilization processes rather than a consistent BDP-induced shift, therefore our hypothesis that the isotopic composition of C would increase in the finer fractions with the BDP dose as effect of enhanced microbial processing, was not corroborated by the results. BDP treatment had no significant effect on $\delta^{15}N$ in the loamy soil, whereas a modest treatment effect was detected in the sandy soil, where P10000 showed higher marginal $\delta^{15}N$ values than P1000.

In general, the changes in isotopic composition of C and N were affected more by the intrinsic soil properties driving C and N transformations than by the addition of the BDP-derived C. In addition, the experimental condition may have reduced the shift in N isotopic composition since our close system did not allow N losses of nitrate. While in an open system the ^{15}N-depleted nitrate may be lost through leaching leaving ^{15}N-enriched ammonium available to microbial biomass, and after several recycling through microorganisms this enriched N may progressively accumulate in the finest aggregate fractions, in our closed system a lack of nitrate loss has probably masked this mechanism.

5 Conclusion

The incorporation of increasing BDP doses for one year in two different soils affected microbial biomass carbon and bacterial and fungal target-gene abundance, aggregate-size distribution, and the allocation of C and N among aggregate fractions. However, these responses depended on both BDP dose and soil characteristics. The highest dose, 1% w/w, by supplying the highest amount of exogenous C, produced the clearest effects, stimulating the MBC, promoting macroaggregate abundance and increasing the associated C and N contents in both soils. The increase in macroaggregates

recovery corresponded to a decrease of the free silt-clay fraction that was partly occluded in the macroaggregates, where C and N are better protected from microbial attack and mineralization. Lower doses had more limited and soil-specific effects, whereas changes in bacterial and fungal abundance were less consistent and depended on soil type and incubation time.

Differently from what hypothesized and despite the measured increase of MBC and bacterial and fungal abundance with the 1% BDP dose, there was no a progressive shift in $\delta^{13}C$ and $\delta^{15}N$ values from coarse to fine aggregate fractions potentially related to microbial C and N transformation and associated to BDP concentration.

After one year of incubation, therefore, the main effects were determined by the 1% BDP dose. This, however, is order of magnitudes higher than the estimated annual input in a real agronomic scenario, therefore the results need to be validated in studies with repeated biodegradable mulch application. On the other hand, the lower doses much closer to real application, are also able to affect some important parameters linked to C and N stabilization and microbial community. Therefore, in perspective, it would be worthwhile to mainly focus on the effects of lower and reliable doses of BDP, together with long-term field studies based on repeated applications to determine whether these effects persist or accumulate over time.

Data availability statement

The original contributions presented in the study are publicly available. This data can be found here: AMS Acta, doi: 10.6092/unibo/amsacta/9137.

Author contributions

PG: Conceptualization, Methodology, Writing – original draft. MM: Data curation, Formal analysis, Writing – original draft. SG: Conceptualization, Investigation, Writing – review & editing. DA: Data curation, Formal analysis, Writing – review & editing. JC: Data curation, Writing – review & editing. DD: Supervision, Writing – review & editing. CM: Funding acquisition, Supervision, Writing – review & editing.

Funding

The author(s) declared that financial support was not received for this work and/or its publication.

Conflict of interest

The author(s) declared that this work was conducted in the absence of any commercial or financial relationships that could be construed as a potential conflict of interest.

The author(s) declared that MM was an editorial board member of Frontiers, at the time of submission. This had no impact on the peer review process and the final decision.

Generative AI statement

The author(s) declared that generative AI was not used in the creation of this manuscript.

Any alternative text (alt text) provided alongside figures in this article has been generated by Frontiers with the support of artificial intelligence and reasonable efforts have been made to ensure accuracy, including review by the authors wherever possible. If you identify any issues, please contact us.

Publisher's note

All claims expressed in this article are solely those of the authors and do not necessarily represent those of their affiliated organizations, or those of the publisher, the editors and the reviewers. Any product that may be evaluated in this article, or claim that may be made by its manufacturer, is not guaranteed or endorsed by the publisher.

Supplementary material

The Supplementary Material for this article can be found online at: https://www.frontiersin.org/articles/10.3389/fsoil.2026.1950823/full#supplementary-material

References

1. Lalitha M, Thilagam V, Balakrishnan N, Mansour M. Effect of plastic mulch on soil properties and crop growth - A review. *Agric Rev*. (2010) 31:145–9.

2. Lee J, Chae HG, Kim GW, Kim PJ, Cho SR. Cover cropping and its biomass incorporation: Not enough to compensate the negative impact of plastic film mulching on global warming. *Sci Total Environ*. (2022) 807:151015. doi: 10.1016/j.scitotenv.2021.151015

3. Steinmetz Z, Wollmann C, Schaefer M, Buchmann C, David J, Tröger J, et al. Plastic mulching in agriculture. Trading short-term agronomic benefits for long-term soil degradation? *Sci Total Environ*. (2016) 550:690–705. doi: 10.1016/j.scitotenv.2016.01.153

4. Xiao L, Wei X, Wang C, Zhao R. Plastic film mulching significantly boosts crop production and water use efficiency but not evapotranspiration in China. *Agric Water Manag*. (2023) 275:108023. doi: 10.1016/j.agwat.2022.108023

5. Xu Z, Zheng B, Yang Y, Yang Y, Jiang G, Tian Y. Effects of biodegradable (PBAT/PLA) and conventional (LDPE) mulch film residues on bacterial communities and

metabolic functions in different agricultural soils. *J Hazard Mater*. (2024) 472:134425. doi: 10.1016/j.jhazmat.2024.134425

6. Chamas A, Moon H, Zheng J, Qiu Y, Tabassum T, Jang JH, et al. Degradation rates of plastics in the environment. *ACS Sustain Chem Eng*. (2020) 8:3494–511. doi: 10.1021/acssuschemeng.9b06635

7. Rillig MC. Microplastic in terrestrial ecosystems and the soil? *Environ Sci Technol*. (2012) 46:6453–4. doi: 10.1021/es302011r

8. PlasticsEurope. Plastics – the Facts 2017. An Analysis of European Plastics Production, Demand and Waste Data (2018). Available online at: https://www.plasticseurope.org (Accessed September 21, 2026).

9. Bodor A, Feigl G, Kolossa B, Mészáros E, Laczi K, Kovács E, et al. Soils in distress: The impacts and ecological risks of (micro)plastic pollution in the terrestrial environment. *Ecotoxicol Environ Saf*. (2024) 269:115807. doi: 10.1016/j.ecoenv.2023.115807

10. Shafea L, Felde VJMNL, Woche SK, Bachmann J, Peth S. Microplastics effects on wettability, pore sizes and saturated hydraulic conductivity of a loess topsoil. *Geoderma*. (2023) 437:116566. doi: 10.1016/j.geoderma.2023.116566

11. Han L, Chen L, Feng Y, Kuzyakov Y, Chen Q, Zhang S, et al. Microplastics alter soil structure and microbial community composition. *Environ Int*. (2024) 185:108508. doi: 10.1016/j.envint.2024.108508

12. Nuñez J, Jiménez-Martínez J, Carminati A, Mitrano DM. Microplastics in agricultural soils: The role of soil texture in modulating oxygen diffusivity and soil respiration. *Soil Biol Biochem*. (2025) 209:109906. doi: 10.1016/j.soilbio.2025.109906

13. Wang S, Wang W, Rong S, Liu G, Li Y, Wang X, et al. Key factors and mechanisms of microplastics' effects on soil nitrogen transformation: A review. *Soil Environ Heal*. (2024) 2:100101. doi: 10.1016/j.seh.2024.100101

14. Boots B, Russell CW, Green DS. Effects of microplastics in soil ecosystems: Above and below ground. *Environ Sci Technol*. (2019) 53:11496–506. doi: 10.1021/acs.est.9b03304

15. Zhao ZY, Wang PY, Wang YB, Zhou R, Koskei K, Munyasya AN, et al. Fate of plastic film residues in agro-ecosystem and its effects on aggregate-associated soil carbon and nitrogen stocks. *J Hazard Mater*. (2021) 416:125954. doi: 10.1016/j.jhazmat.2021.125954

16. Chah CN, Banerjee A, Gadi VK, Sekharan S, Katiyar V. A systematic review on bioplastic-soil interaction: Exploring the effects of residual bioplastics on the soil geoenvironment. *Sci Total Environ*. (2022) 851:158311. doi: 10.1016/j.scitotenv.2022.158311

17. Mazzon M, Gioacchini P, Montecchio D, Rapisarda S, Ciavatta C, Marzadori C. Biodegradable plastics: Effects on functionality and fertility of two different soils. *Appl Soil Ecol*. (2022) 169:104216. doi: 10.1016/j.apsoil.2021.104216

18. Accinelli C, Abbas HK, Bruno V, Nissen L, Vicari A, Bellaloui N, et al. Persistence in soil of microplastic films from ultra-thin compostable plastic bags and implications on soil Aspergillus flavus population. *Waste Manag*. (2020) 113:312–8. doi: 10.1016/j.wasman.2020.06.011

19. Accinelli C, Saccà ML, Mencarelli M, Vicari A. Deterioration of bioplastic carrier bags in the environment and assessment of a new recycling alternative. *Chemosphere*. (2012) 89:136–43. doi: 10.1016/j.chemosphere.2012.05.028

20. Kamiya M, Asakawa S, Kimura M. Molecular analysis of fungal communities of biodegradable plastics in two Japanese soils. *Soil Sci Plant Nutr*. (2007) 53:568–74. doi: 10.1111/j.1747-0765.2007.00169.x

21. Sander M. Biodegradation of polymeric mulch films in agricultural soils: Concepts, knowledge gaps, and future research directions. *Environ Sci Technol*. (2019) 53:2304–15. doi: 10.1021/acs.est.8b05208

22. Degli-Innocenti F, Breton T, Chinaglia S, Esposito E, Pecchiari M, Pennacchio A, et al. Microorganisms that produce enzymes active on biodegradable polyesters are ubiquitous. *Biodegradation*. (2023) 34:489–518. doi: 10.1007/s10532-023-10031-8

23. Liu Y, Zhong Y, Hu C, Xiao M, Ding F, Yu Y, et al. Distribution of microplastics in soil aggregates after film mulching. *Soil Ecol Lett*. (2023) 5(3):230171. doi: 10.1007/s42832-023-0171-9

24. Fojt J, Denková P, Brtnický M, Holátko J, Řezáčová V, Pecina V, et al. Influence of poly-3-hydroxybutyrate micro-bioplastics and polyethylene terephthalate microplastics on the soil organic matter structure and soil water properties. *Environ Sci Technol*. (2022) 56:10732–42. doi: 10.1021/acs.est.2c01970

25. Guggenberger G, Elliott ET, Frey SD, Six J, Paustian K. Microbial contributions to the aggregation of a cultivated grassland soil amended with starch. *Soil Biol Biochem*. (1999) 31:407–19. doi: 10.1016/S0038-0717(98)00143-6

26. Six J, Frey SD, Thiet RK, Batten KM. Bacterial and fungal contributions to carbon sequestration in agroecosystems. *Soil Sci Soc Am J*. (2006) 70:555–69. doi: 10.2136/sssaj2004.0347

27. Yang Y, Dou Y, Wang B, Wang Y, Liang C, An S, et al. Increasing contribution of microbial residues to soil organic carbon in grassland restoration chronosequence. *Soil Biol Biochem*. (2022) 170:108688. doi: 10.1016/j.soilbio.2022.108688

28. Finn D, Kopittke PM, Dennis PG, Dalal RC. Microbial energy and matter transformation in agricultural soils. *Soil Biol Biochem*. (2017) 111:176–92. doi: 10.1016/j.soilbio.2017.04.010

29. Shi J, Wang J, Lv J, Wang Z, Peng Y, Shang J, et al. Microplastic additions alter soil organic matter stability and bacterial community under varying temperature in two contrasting soils. *Sci Total Environ*. (2022) 838:156471. doi: 10.1016/j.scitotenv.2022.156471

30. Werth M, Kuzyakov Y. 13C fractionation at the root-microorganisms-soil interface: A review and outlook for partitioning studies. *Soil Biol Biochem*. (2010) 42:1372–84. doi: 10.1016/j.soilbio.2010.04.009

31. WRB-IUSS. World reference base for soil resources. In: *World Soil Resources Reports 106, World Soil Resources Reports No. 106*. Rome: Food and Agriculture Organization of the United Nations (2015).

32. Scaffaro R, Morreale M, Re GL, Mantia FL. Degradation of Mater-Bi Ò / wood flour biocomposites in active sewage sludge. *Polym Degrad Stab*. (2009) 94:1220–8. doi: 10.1016/j.polymdegradstab.2009.04.028

33. Vance ED, Brookes PC, Jenkinson DS. An extraction method for measuring soil microbial biomass C. *Soil Biol. Biochem*. (1987) 19:703–7. doi: 10.1016/0038-0717(87)90052-6

34. Baffoni L, Alberoni D, Gaggia F, Braglia C, Stanton C, Ross PR, et al. Honeybee exposure to veterinary drugs: How is the gut microbiota affected? *Microbiol Spectr*. (2021) 9(1). doi: 10.1128/spectrum.00176-21

35. Vollmer T, Sto M, Kleesiek K, Dreier J, Icrobiol JCLINM. Evaluation of novel broad-range real-time PCR assay for rapid detection of human pathogenic fungi in various clinical specimens. *J Clin Microbiol*. (2008) 46:1919–26. doi: 10.1128/JCM.02178-07

36. Gioacchini P, Cattaneo F, Barbanti L, Montecchio D, Ciavatta C, Marzadori C. Carbon sequestration and distribution in soil aggregate fractions under Miscanthus and giant reed in the Mediterranean area. *Soil Tillage Res*. (2016) 163:235–42. doi: 10.1016/j.still.2016.06.009

37. Tonon G, Sohi S, Francioso O, Ferrari E, Montecchio D, Gioacchini P, et al. Effect of soil pH on the chemical composition of organic matter in physically separated soil fractions in two broadleaf woodland sites at Rothamsted, UK. *Eur. J. Soil Sci.*. (2010) 61:970–9. doi: 10.1111/j.1365-2389.2010.01310.x

38. R Core Team. *R: A language and environment for statistical computing*. Vienna, Austria: R Foundation for Statistical Computing (2022). Available online at: https://www.R-project.org/.

39. Bandopadhyay S, Martin-Closas L, Pelacho AM, DeBruyn JM. Biodegradable plastic mulch films: Impacts on soil microbial communities and ecosystem functions. *Front Microbiol*. (2018) 9. doi: 10.3389/fmicb.2018.00819

40. Liwarska-Bizukojc E. Effect of (bio)plastics on soil environment: A review. *Sci Total Environ*. (2021) 795:148889. doi: 10.1016/j.scitotenv.2021.148889

41. Rauscher A, Meyer N, Jakobs A, Bartnick R, Lueders T, Lehndorff E. Biodegradable microplastic increases CO2 emission and alters microbial biomass and bacterial community composition in different soil types. *Appl Soil Ecol*. (2023) 182:104714. doi: 10.1016/j.apsoil.2022.104714

42. Zhang H, Yud S, Weiguang L, Wange X, Luf P, Zhang H, et al. Biodegradable mulch films divergently regulate soil carbon cycle by reshaping microbial communities and functional genes. *Journal of Hazardous Materials*. (2026) 506:141616. doi: 10.1016/j.jhazmat.2026

43. Kong M, Huang MJ, Zhang ZX, Long J, Siddique KHM, Zhang DM. Effects of plastic film mulching on soil microbial carbon metabolic activity and functional diversity at different maize growth stages in cool, semi-arid regions. *Front Microbiol*. (2024) 15:1492149. doi: 10.3389/fmicb.2024.1492149

44. Guliyev V, Tanunchai B, Noll M, Buscot F, Purahong W, Blagodatskaya E. Links among microbial communities, soil properties and functions: Are fungi the sole players in decomposition of bio-based and biodegradable plastic? *Polymers (Basel)*. (2022) 14:2801. doi: 10.3390/polym14142801

45. Liu H, Yang X, Liu G, Liang C, Xue S, Chen H, et al. Response of soil dissolved organic matter to microplastic addition in Chinese loess soil. *Chemosphere*. (2017) 185:907–14. doi: 10.1016/j.chemosphere.2017.07.064

46. Zhou J, Jia R, Brown RW, Yang Y, Zeng Z, Jones DL, et al. The long-term uncertainty of biodegradable mulch film residues and associated microplastics pollution on plant-soil health. *J Hazard Mater*. (2023) 442:130055. doi: 10.1016/j.jhazmat.2022.130055

47. Bandopadhyay S, Liquet y González JE, Henderson KB, Anunciado MB, Hayes DG, DeBruyn JM. Soil microbial communities associated with biodegradable plastic mulch films. *Front Microbiol*. (2020) 11. doi: 10.3389/fmicb.2020.587074

48. Song D, Jin G, Su Z, Ge C, Fan H, Yao H. Influence of biodegradable microplastics on soil carbon cycling: Insights from soil respiration, enzyme activity, carbon use efficiency and microbial community. *Environ Res*. (2025) 266:120558. doi: 10.1016/j.envres.2024.120558

49. Zhou A, Ji Q, Kong X, Zhu F, Meng H, Li S, et al. Response of soil property and microbial community to biodegradable microplastics, conventional microplastics and straw residue. *Appl Soil Ecol*. (2024) 196:105302. doi: 10.1016/j.apsoil.2024.105302

50. Wagner S, Cattle SR, Scholten T. Soil-aggregate formation as influenced by clay content and organic-matter amendment. *J Plant Nutr Soil Sci*. (2007) 170:173–80. doi: 10.1002/jpln.200521732

51. Zhang GS, Zhang FX, Li XT. Effects of polyester microfibers on soil physical properties: Perception from a field and a pot experiment. *Sci Total Environ*. (2019) 670:1–7. doi: 10.1016/j.scitotenv.2019.03.149

52. De Souza MacHado AA, Lau CW, Till J, Kloas W, Lehmann A, Becker R, et al. Impacts of microplastics on the soil biophysical environment. *Environ Sci Technol*. (2018) 52:9656–65. doi: 10.1021/acs.est.8b02212

53. Tang KHD. Microplastics in agricultural soils in China: Sources, impacts and solutions. *Environmental Pollution*. (2023) 322:121235. doi: 10.1016/j.envpol.2023.121235

54. Rillig MC, Ingraffia R, De Souza Machado AA. Microplastic incorporation into soil in agroecosystems. *Front Plant Sci*. (2017) 8. doi: 10.3389/fpls.2017.01805

55. King AE, Congreves KA, Deen B, Dunfield KE, Voroney RP, Wagner-Riddle C. Quantifying the relationships between soil fraction mass, fraction carbon, and total soil carbon to assess mechanisms of physical protection. *Soil Biol Biochem*. (2019) 135:95–107. doi: 10.1016/j.soilbio.2019.04.019

56. Six J, Elliott ET, Paustian K. Soil macroaggregates turnover and microaggregate formation: a mechanism for C sequestration under no-tillage agriculture. *Soil Biol. Biochem.*. (2000) 32:2099–103. doi: 10.1016/S0038-0717(00)00179-6

57. Hurley RR, Nizzetto L. Fate and occurrence of micro(nano)plastics in soils: Knowledge gaps and possible risks. *Curr Opin Environ Sci Heal*. (2018) 1:6–11. doi: 10.1016/j.coesh.2017.10.006

58. Plaza C, Gollany HT, Baldoni G, Polo A, Ciavatta C. Predicting long-term organic carbon dynamics in organically amended soils using the CQESTR model. *J Soils Sediments*. (2012) 12:486–93. doi: 10.1007/s11368-012-0477-1

59. Angst G, Mueller KE, Kögel-Knabner I, Freeman KH, Mueller CW. Aggregation controls the stability of lignin and lipids in clay-sized particulate and mineral associated organic matter. *Biogeochemistry*. (2017) 132:307–24. doi: 10.1007/s10533-017-0304-2

60. Kirchmann H, Haberhauer G, Kandeler E, Sessitsch A, Gerzabek MH. Effects of level and quality of organic matter input on carbon storage and biological activity in soil: Synthesis of a long-term experiment. *Global Biogeochem Cycles*. (2004) 18:1–9. doi: 10.1029/2003GB002204

61. Matus FJ. Fine silt and clay content is the main factor defining maximal C and N accumulations in soils: a meta-analysis. *Scientific Reports*. (2021) 11:6438. doi: 10.1038/s41598-021-84821-6

62. Stewart CE, Plante AF, Paustian K, Conant RT, Six J. Soil Carbon Saturation: Linking Concept and Measurable Carbon Pools. *Soil Sci. Soc. Am. J.*. (2008) 72:379–92. doi: 10.2136/sssaj2007.0104

63. Christensen BT. Physical fractionation of soil and structural and functional complexity in organic matter turnover. *European J. Soil Sci.*. (2001) 52:345–53. doi: 10.1046/j.1365-2389.2001.00417.x

64. De Clercq T, Heiling M, Dercon G, Resch C, Aigner M, Mayer L, et al. Predicting soil organic matter stability in agricultural fields through carbon and nitrogen stable isotopes. *Soil Biol Biochem*. (2015) 88:29–38. doi: 10.1016/j.soilbio.2015.05.011